J. Mt. Sci. (2016) 13(11): 2069-2078 e-mail: jms@imde.ac.cn http://jms.imde.ac.cn
DOI: 10.1007/s11629-016-4001-8

A new method for the stability analysis of geosynthetic-reinforced slopes

SONG Fei[1] http://orcid.org/0000-0001-5804-5576; e-mail: songf1980@163.com

CHEN Ru-yi[1] http://orcid.org/0000-0002-0000-1666; e-mail: 947522468@qq.com

MA Li-qiu[2*] http://orcid.org/0000-0002-1640-1859; e-mail: lqmo_912@163.com

CAO Geng-ren[3] http://orcid.org/0000-0002-6342-1270; e-mail: caogengren@cmhk.com

**Corresponding author*

1 Institute of Geotechnical Engineering, School of Highway Engineering, Chang'an University, Xi'an 710064, China

2 Guizhou Electricity Engineering Construction Supervise Company, Guiyang 550005, China

3 Merchants Chongqing Communications Research and Design Institute Co., Ltd., Chongqing 400067, China

Citation: Song F, Chen RY, Ma LQ, et al. (2016) A new method for the stability analysis of geosynthetic-reinforced slopes. Journal Mountain Science 13(11). DOI: 10.1007/s11629-016-4001-8

© Science Press and Institute of Mountain Hazards and Environment, CAS and Springer-Verlag Berlin Heidelberg 2016

Abstract: This paper is concerned with the stability analysis of reinforced slopes. A new approach based on the limit equilibrium principle is proposed to evaluate the stability of the reinforced slopes. The effect of reinforcement is modeled as an equivalent restoring force acting the bottom of the slice and added into the general limit equilibrium (GLE) method. The equations of force and moment equilibrium of the slice are derived and corresponding iterative solution methods are provided. The new method can satisfy both the force and the moment equilibrium and be applicable to the critical failure surface of arbitrary form. Furthermore, the results predicted by the proposed method are compared with the calculation examples of other researchers and the centrifuge model test results to validate its correctness and effectiveness.

Keywords: Reinforced slope; Stability analysis; Limit equilibrium; General limit equilibrium method; Centrifuge model test

Received: 20 April 2016
Accepted: 30 August 2016

Introduction

In recent years, geosynthetic-reinforced soil structures, such as slopes, embankments and retaining walls are widely used in China and elsewhere due to the increasing infrastructural development demands, as is shown in Figure 1. Construction of slopes at steeper angles can be realized by the use of geosynthetics, thereby decreasing land requirements for slope construction. The stability analysis of reinforced slopes can be conducted using the limit equilibrium method. Leshchinsky and Reinschmidt (1985), Leshchinsky and Boedeker (1989) presented an analytical approach for the stability analysis of reinforced slopes based on limit equilibrium theory. In the analysis, the failure surfaces are either log-spiral or bilinear and two extreme inclinations of reinforcement force are investigated: tangential to the slice base and horizontal. Rowe and Soderman (1985) extended the simplified Bishop slip circle method by incorporating the reinforcement effect and estimated the stability of geotextile-reinforced

Figure 1 Photo of a geosynthetic-reinforced slope (in Beijing-Chengde highway, taken by Tensar Geosynthetics Limited Company in 2009).

embankments. Sabhahit et al. (1994) conducted the stability analysis of a reinforced embankment constructed on a non-homogeneous clay deposit of finite depth by modifying Janbu's generalized procedure of slices. Shahgholi et al. (2001) presented horizontal slice method for the stability analysis of reinforced slope. Some researchers performed stability analysis of slopes using finite element method (FEM). Griffiths and Lane (1999), Dawson et al. (1999) conducted stability analysis of slopes by means of shear strength reduction technique in finite element method (FEM). Mehdipour et al. (2013) calculated the factor of safety and the location of failure surface of geocell reinforced slope using the strength reduction method by employing the finite difference program FLAC 2D. Although FEM can be applied to a lot of complex conditions, the accuracy of the results depends greatly on the appropriate constitutive model adopted in the analysis. In addition, in many practical situations, its sophistication cannot be warranted due to the insufficiency of time and fund. Therefore, among the many approaches, limit equilibrium method is still very popular and generally preferred for the stability analysis of reinforced slopes because of its simplicity, accuracy and familiarity for engineers. The limit equilibrium techniques for unreinforced slopes have been modified and extended to incorporate the effect of reinforcement by a lot of researchers. However, some approaches have the limitations of the shapes of failure surfaces. For example, the method of Jewell (1991) can only be suitable for bilinear failure surfaces. Leshchinsky and Boedeker (1989) assumed logarithmic spiral failure mechanism in the analysis. Besides, the circular failure surfaces were adopted by Hird (1986), Wright and Duncan (1991), Mandal and Labhane (1992), Mandal and Joshi (1996), Palmeira et al. (1998). In addition, some methods can only satisfy moment equilibrium such as those extended from the simplified Bishop slip circle analysis (Rowe and Soderman 1985), while others can only satisfy force equilibrium such as those extended from the Janbu's method (Greenwood 1990; Sabhahit et al. 1994).

In this paper, a new rigorous approach satisfying both force and moment equilibrium is proposed to evaluate the stability of geosynthetic-reinforced slope by the extension of general limit equilibrium (GLE) method (Fredlund and Krahn 1977; Fredlund et al. 1981; Chugh 1986; Zhang 2005). The proposed method can be applied to both circular and arbitrary polygonal shape. The effectiveness of the method is confirmed by the comparison with other researchers and the centrifuge model test results.

1 Formulation of the Method

1.1 Determination of the reinforcing force

According to the pullout test results of Mitchell and Christopher (1990), the pullout resistance of the geosynthetic material can be estimated by the following equation:

$$t = 2 \cdot k \cdot \tan\varphi \cdot \bar{\sigma}_v \cdot l_e \quad (1)$$

where t=the pullout resistance per unit width of geosynthetic sheet; k= a parameter related to the coefficient of friction at the interface between the soil and the geosynthetic material (within the range of 0.6～1.0); φ = the internal friction angle of the soil; $\bar{\sigma}_v$ = average normal stress along the embedment length; l_e = the embedment length beyond the failure surface.

In order to be conservative in the design in engineering practices, a factor of safety is introduced to present the mobilized pullout resistance of the geosynthetic material by the following equation:

$$t_m = 2 \cdot k \cdot \tan\varphi_m \cdot \overline{\sigma_v} \cdot l_e = 2 \cdot k \cdot (\tan\varphi / F_g) \cdot \overline{\sigma_v} \cdot l_e \quad (2)$$

where t_m = mobilized pullout resistance of the

geosynthetic sheet; F_g= a factor of safety defining the mobilized strength of frictional soil.

The average normal stress along the embedment length beyond the failure surface can be obtained by the following equation:

$$\bar{\sigma}_v = \gamma \cdot \bar{h}_p + p \tag{3}$$

where γ=the unit weight of the soil; $\bar{h}_p$ = the average height of the soil slices above the geosynthetic sheet beyond the failure surface; p = the surcharge acting on the surface of the slope.

In the limit equilibrium analysis, the reinforcing force provided by the geosynthetic sheet at the bottom of each slice, denoted as T, can be determined by comparing the pullout resistance obtained by Eq. (2) with the tensile strength of the fabric, represented by T_g. The value of T is the smaller one of t_m and T_g and its unit is kN/m.

1.2 Equations of force and moment equilibrium

The soil mass inside the failure surface is divided into n slices. When dividing the soil mass into slices, the intersection point of the geosynthetic sheet with the base of the slice is selected as the midpoint of the slice at the location of the reinforcement, which is illustrated in Figure 2.

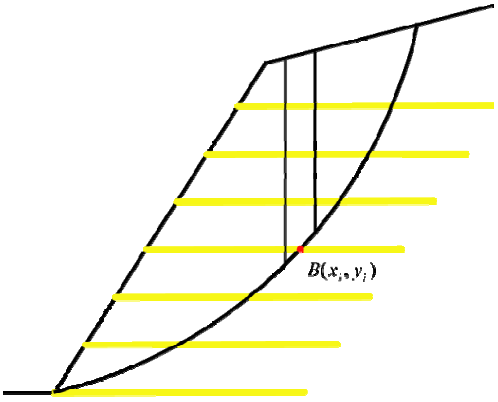

Figure 2 Division of potential sliding mass into slices.

The vertical slice taken from the slope and the forces acting on it is illustrated in Figure 3. Force equilibrium is considered in a direction parallel to the base of each slice in the following equation:

$$\tau_{mi} + Z_{Li}\cos(\alpha_i - \theta_{Li}) - Z_{Ri}\cos(a_i - \theta_{Ri}) - W_i \sin\alpha_i + T_i \cos(\alpha_i - \eta_i) - pl_i \sin(\alpha_i - \beta_i) = 0 \tag{4}$$

where Z_{Li} and Z_{Ri} are the inter-slice resultant forces on the left and right side of the ith slice. θ_{Li} and θ_{Ri} are the left and right inter-slice force angle. α_i is the angle between the base of the ith slice and the horizontal. W_i is the weight of the ith slice. T_i is the reinforcing force provided by the geosynthetic sheet at the base of the ith slice. l_i is the length of the base of the ith slice, as is shown in Figure 4. β_i is the angle between the top of the slice and the horizontal.

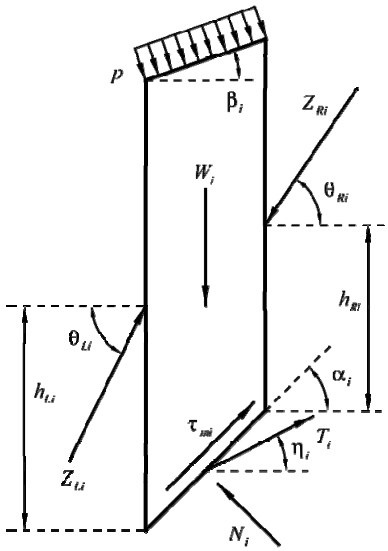

Figure 3 Schematic diagram of forces acting on the slice.

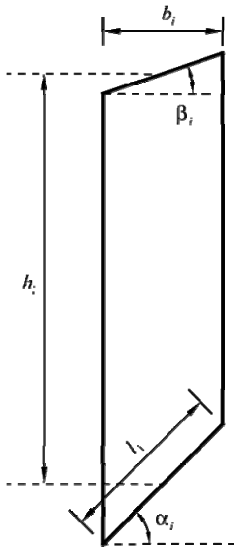

Figure 4 Geometric size of the slice.

η_i is the angle between the action direction of T_i and the horizontal and can be determined by the following equation:

$$\eta_i = \mu\alpha_i \tag{5}$$

where μ is a parameter representing the direction of Ti and its range is 0～1, thereby, the variation of η_i is within the range of 0～α_i. On one hand, when μ=0, the action direction of T_i is horizontal. Although it produces a smaller stabilizing moment, the increase of normal force at slice base due to the reinforcement in turn increases the frictional resistance of soil. On the other hand, when μ=1, the action direction of T_i is tangential to the base of the slice. Although a reinforcement force tangential to the slice base may produce a larger stabilizing moment than the horizontal force, it does not increase the normal forces along the failure surface (Zornberg et al. 1998b).

It should be noted that in this study all the angles are positive when they rotate clockwise from the horizontal but are negative when they rotate anti-clockwise from the horizontal.

τ_{mi} is the mobilized strength and can be determined by the following equation according to the Mohr-Coulomb strength criterion adopted in the analysis:

$$\tau_{mi} = \frac{\tau_i}{F} = \frac{cl_i + N_i \tan\varphi}{F} = c_{mi} + N_i \tan_m \qquad (6)$$

where c and φ are the cohesion and internal friction angle of the soil. F is the factor of safety of the slope. N_i is the normal force to the base of the ith slice.

Then by substituting Equation (6) into (4), the following expression is derived:

$$N_i \tan\varphi_m = Z_{Ri}\cos(\alpha_i - \theta_{Ri}) - Z_{Li}\cos(\alpha_i - \theta_{Li}) + W_i \sin\alpha_i - c_{mi} - T_i \cos(\alpha_i - \eta_i) + pl_i \sin(\alpha_i - \beta_i) \qquad (7)$$

Next force equilibrium is formulated in a direction normal to the base of the slice:

$$N_i = Z_{Ri}\sin(\theta_{Ri} - \alpha_i) - Z_{Li}\sin(\theta_{Li} - \alpha_i) + W_i \cos\alpha_i - T_i \sin(\alpha_i - \eta_i) + pl_i \cos(\alpha_i - \beta_i) \qquad (8)$$

By substituting Equation (8) into (7), the following force equilibrium equation can be formulated:

$$Z_{Ri} = A_{8i} Z_{Li}\left[\cos(\alpha_i - \theta_{Li}) + \sin(\alpha_i - \theta_{Li})\tan\varphi_m\right] + A_{8i}\{W_i \cos\alpha_i \left(\tan\varphi_m - \tan\alpha_i\right) + c_{mi} + T_i \cos\left(\alpha_i - \eta_i\right)\left[1 - \tan(\alpha_i - \eta_i)\tan\varphi_m\right] + pl_i \cos(\alpha_i - \beta_i)\left[\tan\varphi_m - \tan(\alpha_i - \beta_i)\right]\} \qquad (9)$$

where $A_{8i} = \dfrac{1}{\cos(\alpha_i - \theta_{Ri})[1 + \tan\varphi_m \tan(\alpha_i - \theta_{Ri}]}$ (10)

The overall moment equilibrium of the forces about the midpoint of base of the slice is given by:

$$Z_{Li}\cos\theta_{Li}\left(h_{Li} - \frac{b_i}{2}\tan\alpha_i\right) + Z_{Li}\frac{b_i}{2}\sin\theta_{Li} - Z_{Ri}\cos\theta_{Ri}\left(h_{Ri} + \frac{b_i}{2}\tan\alpha_i\right) + Z_{Ri}\frac{b_i}{2}\sin\theta_{Ri} + pl_i\cos(\alpha_i - \beta_i)h_i\sin\alpha_i - pl_i\sin(\alpha_i - \beta_i)h_i\cos\alpha_i = 0 \qquad (11)$$

By simplifying Eq. (11) the location of the inter-slice force on the right side of the ith slice, h_{Ri}, can be obtained:

$$h_{\mathrm{Ri}} = \frac{Z_{\mathrm{Li}}}{Z_{\mathrm{Ri}}\cos\theta_{\mathrm{Ri}}}\left[h_{\mathrm{Li}}\cos\theta_{\mathrm{Li}} - \frac{b_i}{2}(\cos\theta_{\mathrm{Li}}\tan\alpha_i - \sin\theta_{\mathrm{Li}})\right] + \frac{b_i}{2}(\tan\theta_{Ri} - \tan\alpha_i) + \frac{pl_i h_i \cos(\alpha_i - \beta_i)\cos\alpha_i[\tan\alpha_i - \tan(\alpha_i - \beta_i)]}{Z_{Ri}\cos\theta_{Ri}} \qquad (12)$$

where h_{Li} and h_{Ri} are the height to forces Z_{Li} and Z_{Ri} respectively. b_i is the width of the slice, which is demonstrated in Figure 4.

As is known to all, the number of the above formulated equations is 4n. However, the number of total unknowns is 5n-2. Therefore, additional n-2 assumptions are required to make the problem determinate. As is treated in the same way with the GLE method (Fredlund and Krahn 1977; Fredlund et al. 1981; Chugh 1986; Zhang 2004), the inter-slice force angle is assumed in the following expression:

$$\theta = \lambda f(x) \qquad (13)$$

where θ is the inter-slice force angle and its number is n-1. The inter-slice force angle for the left side of the first slice and the right side of the last slice is assumed to be zero. Because each θ has the same value of λ, only n-2 independent unknowns have been assumed. Then the number of unknowns and the equations are the same. Different limit equilibrium methods can be formulated when inter-slice force angle function, $f(x)$, is assumed in various forms. For example, if $f(x)$ = 1, it is Spencer's Procedure. For Morgenstern-Price method, $f(x)$ takes various forms of function, such as half-sine, clipped-sine, and so on. In this study, $f(x)$ is assumed to be a half-sine function in the following expression:

$$f(x) = \sin\left[\left(\frac{x-a}{b-a}\right)\pi\right] \qquad (14)$$

where x is the horizontal coordinate of the inter-

slice force, a and b are the horizontal coordinates of the toe and the crest of the slope, respectively.

1.3 Iteration procedure

The iteration procedure for the proposed new method is as follows:

(1) The value of λ and the iterative initial value of the factor of safety are selected. The factor of safety obtained by the transmission method of unbalanced thrust is usually taken as the iterative initial value of the proposed method. Z_{L_1} and h_{L_1} i.e. , Z_L and h_L of the first slice at the toe of the slope are both zero. Z_{R_1} and h_{R_1} can be calculated by Eq. (9) and (12) and are taken as Z_{L2} and h_{L_2}. These calculations are performed sequentially for each slice until Z_{Rn} and h_{Rn}, i.e., Z_R and h_R of the last slice on the crest of the slope are got.

(2) If all the forces satisfy the force equilibrium, $Z_{Rn}=0$. At this time the factor of safety satisfying the force equilibrium is denoted as F_f. Otherwise, the value of F is adjusted and Z_{Ri} is calculated according to Eq. (9) until $Z_{Rn}=0$ and F_f can be determined. In the same way, if all the forces satisfy the moment equilibrium, $h_{Rn}=0$. At this time the factor of safety satisfying the moment equilibrium is denoted as F_m. Otherwise, the value of F is adjusted and h_{Ri} is calculated according to Eq. (12) until $h_{Rn}=0$ and F_m can be determined. A tolerable limit, $\varepsilon \le 10^{-3}$, is prescribed when judging whether Z_{Rn} and h_{Rn} equal zero. It should be noted that λ maintains the same value in this step and two points $(\tan\lambda, F_f)$ and $(\tan\lambda, F_m)$ can be determined.

(3). Change the value of λ and repeat the steps of (2) and (3) and another group of $(\tan\lambda, F_f)$ and $(\tan\lambda, F_m)$ can be got. The range of λ is usually from 0° to 120°. It should be guaranteed that $\theta = \lambda f(x) < 90^\circ$.

(4). $(\tan\lambda, F_f)$ and $(\tan\lambda, F_m)$ corresponding to different λ values are computed. Force equilibrium line is plotted by connecting all the points of $(\tan\lambda, F_f)$ in the $\tan\lambda - F$ coordinate system. Similarly, moment equilibrium line can be got in the same way by connecting all the points of $(\tan\lambda, F_m)$ in the $\tan\lambda - F$ coordinate system. The ordinate of intersection point of the two lines is the factor of safety that satisfies both force and moment equilibrium.

It should be noted that the factor of safety calculated by the above procedure is the one for a fixed failure surface. The smallest factor of safety corresponding to the critical failure surface can be searched by the exhaustive method for the arch failure surface or the improved Monte Carlo techniques proposed by Zhang et al. (2006a, 2006b and 2006c) for the non-arch failure surface.

2 Analysis of Calculation Examples

The corresponding code is written for the stability analysis of geosyntehtic-reinforced slope according to the above procedure and added into the program, ZSLOPE, developed by Zhang (2004). The geometric model in the calculation is shown in Figure 5. Both circular and polygonal line failure surfaces are employed in the analysis. The parameters of the uniform soil slope are: $c = 20kPa$, $\varphi = 35^\circ$, $\gamma = 18kN/m^3$. The tensile strength of the geosynthetic sheet is 50 kN/m. The reinforcement length has been extended beyond the failure surface and the force direction is horizontal.

The calculation of the factor of safety of the circular and polygonal line failure surface is shown in Figures 6 and 7 respectively. It can be observed from Figures 6 and 7 that intersection point of the line F_f and F_m is the factor of safety and the

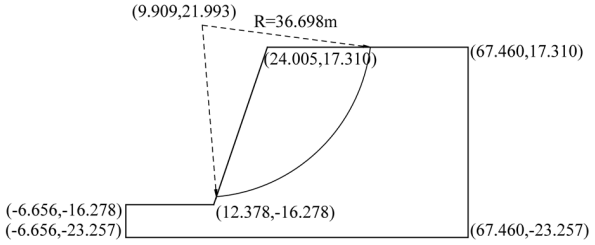

(a) Circular failure surface

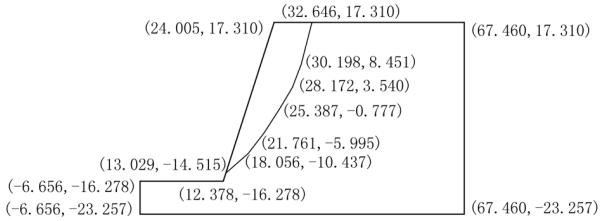

(b) Polygonal Line failure surface

Figure 5 Geometric size of the calculation model (unit: m).

corresponding $\tan\lambda$ satisfying both force and moment equilibrium. The factor of safety of the reinforced slope is somewhat higher than that of the unreinforced slope.

3 Comparison with Other Examples

In order to verify the effectiveness of the proposed method, the prediction results of this method is compared with those of the calculation examples of Borges and Cardoso (2002) and Tandjiria et al. (2002). According to Borges and Cardoso (2002), the geometric size of the model is shown in Figure 8. The unit weight, internal friction angle and cohesion of the sand are 21.9 kN/m³, 35°and 0 kPa, respectively. The material properties of the layered foundation are listed in

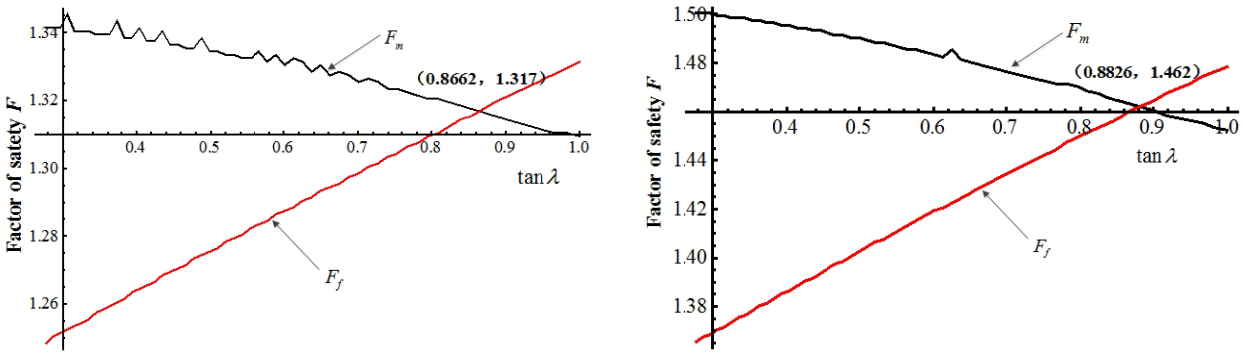

(a) Unreinforced slope (b) Reinforced slope

Figure 6 Iteration process for the factor of safety of the slope with circular failure surface.

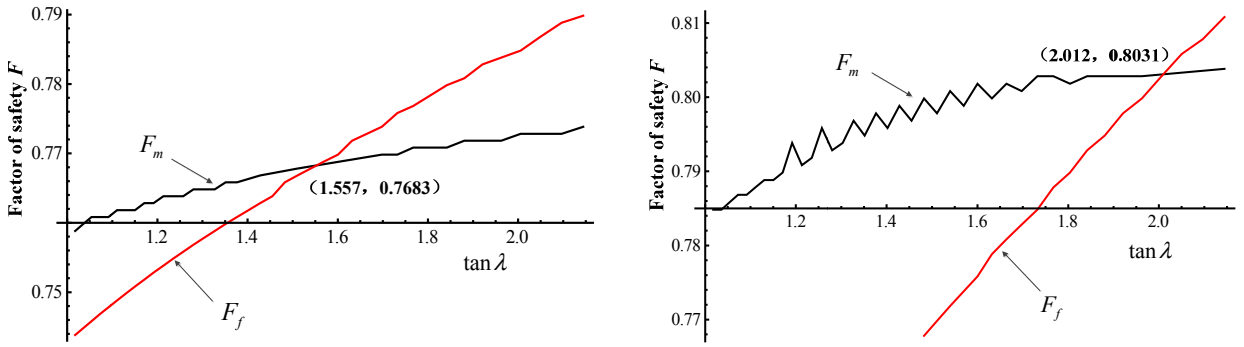

(a) Unreinforced slope (b) Reinforced slope

Figure 7 Iteration process for the factor of safety of the slope with polygonal line failure surface.

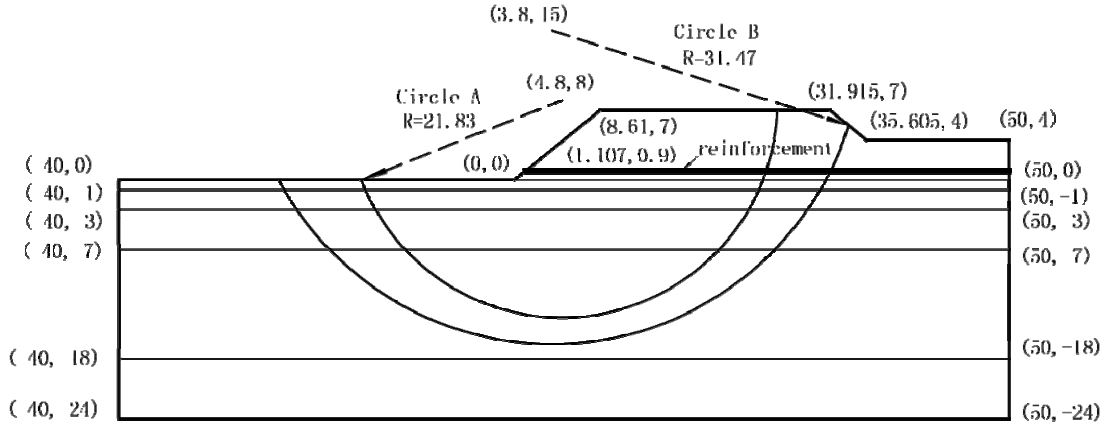

Figure 8 Geometric size of the calculation model of Borges and Cardoso (2002) (Unit: m).

Table 1. In addition, the mechanical parameters of the reinforcement are: T_g = 200 kN/m, μ = 0 and F_g = 1.167. In this example, the problem is to search for the factor of safety corresponding to the prescribed failure surfaces, i.e., Circle A and B, illustrated in Figure 8.

Taking Circle A for example, the calculation model formulated in ZSLOPE is shown in Figure 9. Due to the length restriction, the model of Circle B is not given here. The comparison of the factors of safety predicted by the proposed method and those of Borges and Cardoso (2002) is made. The factors of safety of Circle A and B predicted by the proposed method are 1.20 and 1.19, respectively. At the same time, the factors of safety of Circle A and B calculated by Borges and Cardoso (2002) are 1.25 and 1.19, respectively. The little differences between the calculation results of the proposed method and those of Borges and Cardoso (2002) demonstrate its precision and accuracy.

Another comparison is made between the prediction results of the method in this study and those of Tandjiria et al. (2002). The geometric size of the model of Tandjiria et al. (2002) is shown in Figure 10 and the properties of the embankment and the foundation are listed in Table 2. The mechanical parameters of the reinforcement are: T_g = 44 kN/m, k = 0.6, μ = 0 and F_g = 1.35. In this example, the problem is to search for the smallest safety factor and the corresponding critical failure surface. The factor of safety predicted by the proposed method is 1.31, which is close to 1.35, provided by Tandjiria et al. (2002), showing the effectiveness of the proposed method.

Table 1 Parameters of Clay in the model of Borges and Cardoso (2002)

Material	Cohesion of the soil c_u (kPa)	Unit weight of the soil $\gamma(kN/m^3)$
Clay1	43	18
Clay2	31	16.6
Clay3	30	13.5
Clay4	32	17
Clay5	32	17.5

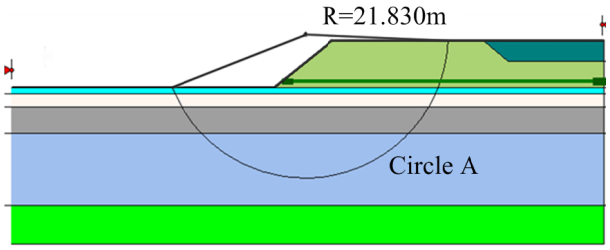

Figure 9 Calculation model of Circle A formulated by software ZSLOPE (Zhang 2004).

Table 2 Parameters of sand and clay in the model of Tandjiria et al. (2002)

Material	Cohesion of the soil c'/c_u (kPa)	Internal friction angle of the soil $\varphi'(\circ)$	Unit weight of the soil $\gamma(kN/m^3)$
Sand Fill	0	37	17
Soft Clay	20	0	19.4

Table 3 Parameters of soil in the centrifuge model tests of Zornberg et al. (1998)

	Cohesion of the soil c' (kPa)	Internal friction angle of the soil $\varphi'(\circ)$	Unit weight of the soil $\gamma(kN/m^3)$
Model B6, B9 and S6	0	39.5	15.64
Model D6	0	42.5	16.21

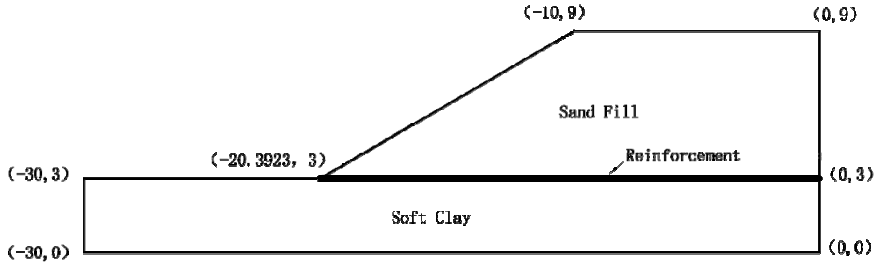

Figure 10 Geometric size of the calculation model of Tandjiria et al. (2002) (Unit: m).

4 Verification with Centrifuge Model Test Results

The centrifuge model tests of Zornberg et al. (1998) are calculated by the proposed method and the prediction results are compared with the measured one in order to verify the correctness and effectiveness of the method. The geometric sizes of Model B6, B9, D6 and S6 are shown in Figure 11. Tables 3 and 4 present the conditions and material properties of Model B6, B9, D6 and S6. The failure surface and the factor of safety of Model B6, B9, D6 and S6 at failure are

Table 4 Parameters of reinforcement in the centrifuge model tests of Zornberg et al. (1998)

Parameters	B6	B9	D6	S6
Number of reinforcement layers	6	9	6	6
Vertical spacing (mm)	38.1	25.4	38.1	38.1
Length of reinforcement layer (mm)	203	203	203	203
g-level at failure	21	37	29	32
T_g (kN/m)	0.123	0.123	0.123	0.183
k	0.9	0.9	0.9	0.9
F_g	1.2	1.2	1..2	1.2
μ	0	0	0	0

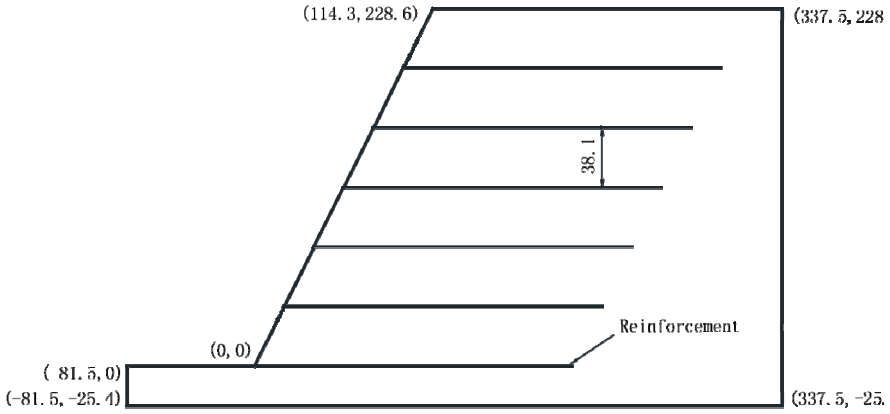

(a) Model B6, D6 and S6

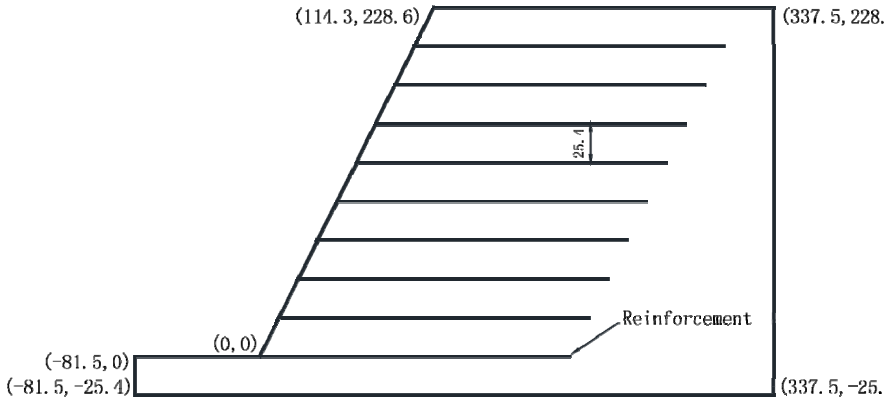

(b) Model B9

Figure 11 Geometric size of Model B6, D6, S6 and B9 in the centrifuge model tests of Zornberg et al. (Unit: mm).

predicted by the proposed method. The failure surfaces predicted by the proposed method are in good agreement with those measured in the centrifuge model tests of Zornberg et al. (1998), as is shown in Figure 12, confirming the effectiveness of the method. The factors of safety of Model B6, B9, D6 and S6 at failure calculated by the proposed method are 0.92, 0.88, 0.90 and 0.91, respectively. It can be observed that the calculated factors of safety at failure are near 1, showing the correctness of the method. In addition, the analytical failure mode of the geotextile is also studied and compared with that in the centrifuge model tests. According to the geometric size in Figure 11, the location of the calculated critical failure surface, γ in Table 3 and g-level at failure in Table 4, $\overline{\sigma}_v$ is obtained by Eq. (3). By substituting the calculated $\overline{\sigma}_v$ and the corresponding parameters in Table 3 and 4 into Eq. (2), the mobilized pullout resistance is calculated and compared with the geotextile tensile strength. The pullout resistance is found to be much larger than the geotextile tensile strength at the failure acceleration in the centrifuge tests. Therefore, the failure mode of the geotextile is tie-break, which is the same with that has been reported by Zornberg et al. (1998a), i.e., the reinforcement layers failed by breakage instead of pullout when intersected by the failure surfaces.

5 Conclusions

In this paper, the GLE method is modified and extended to incorporate the reinforcement effect for the stability analysis of geosynthetic-reinforced slopes. Based on the force equilibrium in the direction parallel and normal to the slice base and the moment equilibrium at the center of the slice base, the corresponding equations are derived. The issue of static indetermination is addressed by introducing a half-sinusoidal function for the inclination of inter-slice forces. After that, iterative solution methods for obtaining the factor of safety which satisfies both

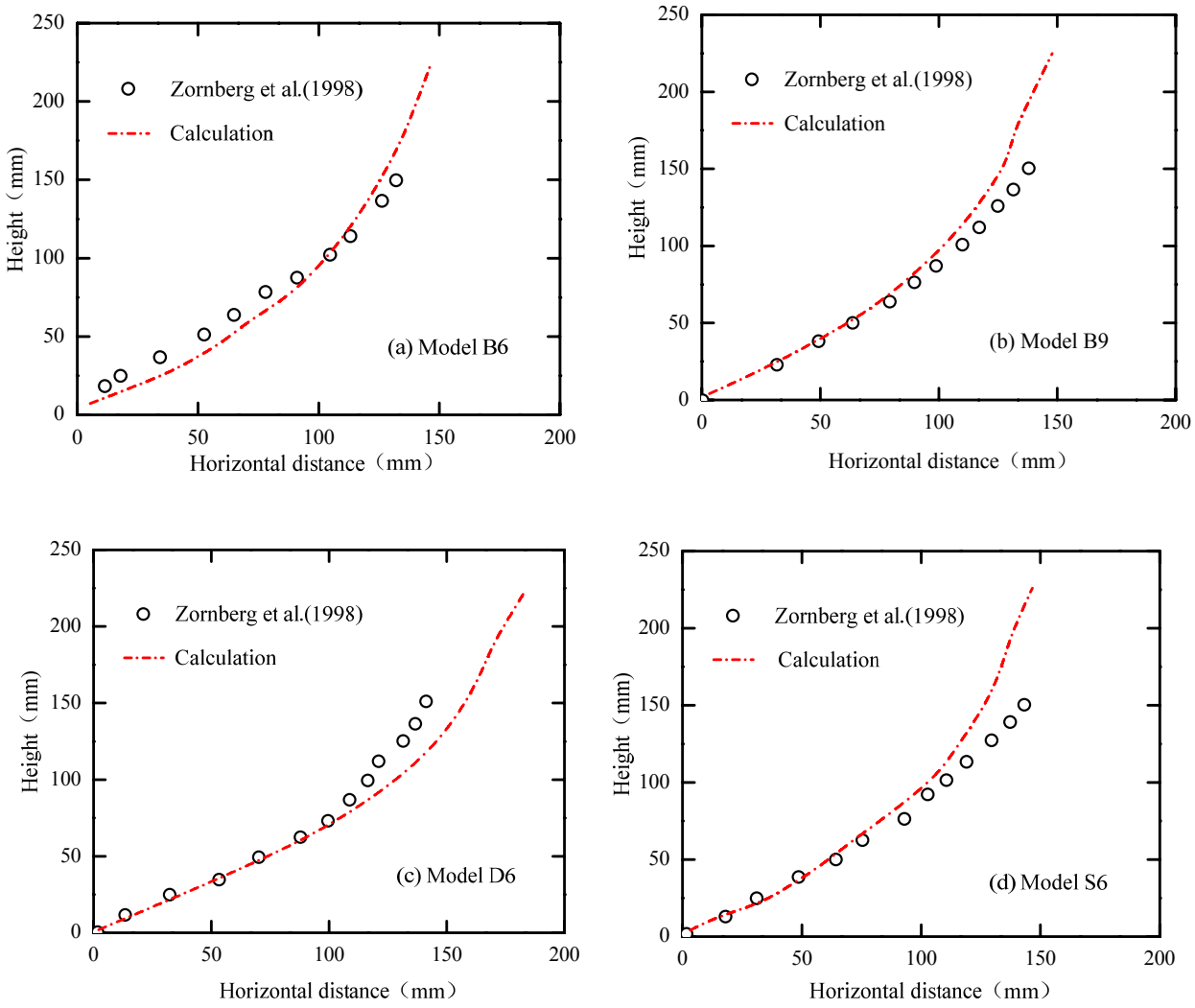

Figure 12 Comparison of predicted failure surfaces with the test results of Zornberg et al. (1998).

force and moment equilibrium are provided. The new method is more rigorous than the existing methods in use and be applicable to the failure surface of arbitrary form, including both arch and polygonal line. Furthermore, the effectiveness of the proposed method is validated by the examples of other researchers and the centrifuge model test results of Zornberg et al. (1998). Parametric studies will be conducted to investigate the effects of some factors, such as the tensile strength of reinforcement, the orientation of the tensile force, the length of reinforcement, the spacing of reinforcing layers on the factor of safety and critical failure surface of slopes in the future study.

Acknowledgements

This study was funded by the Key Industrial Science and Technology Project of Shaanxi Province (No. 2015GY149) and the Scientific Project funded by the Ministry of Housing and Urban-Rural Development of the People's Republic of China Council (No. 2015-K2-008). Special thanks were given to Dr. Lu-Yu Zhang for his kind help in writing the program.

References

Borges JL, Cardoso AS (2002) Overall stability of geosynthetic-reinforced embankments on soft soils. Geotextiles and Geomembranes 20(6): 395-421. DOI: 10.1016/S0266-1144(02)00014-6

Chugh AK (1986) Variable interslice force inclination in slope stability analysis. Soils and Foundations 26(1): 115-121. DOI: 10.3208/sandf1972.26.115

Dawson EM, Roth WH, Drescher A (1999) Slope stability analysis by strength reduction. Geothchnique 49(6): 835-840. DOI: http://dx.doi.org/10.1680/geot.1999.49.6.835

Fredlund DG, Krahn J (1977) Comparison of slope stability methods of analysis. Canadian Geotechnical Journal 14(3):429-439. DOI: 10.1139/t77-045

Fredlund DG, Krahn J, Pufahl DE (1981) The relationship between limit equilibrium slope stability methods. In proceedings of the 10th ICSMFE, Stockholm, Sweden. 3: 409-416. DOI: 10.1016/0148-9062(84)91799-6

Greenwood JR (1990) Design approach for slope repairs and embankment widening. In: Shercliff, DA (Ed.), Reinforced Embankments: Theory and Practice. Thomas Telford, London.

Griffiths DV, Lane PA (1999) Slope stability analysis by finite elements. Geotechnique 49(3): 387-403. DOI: 10.1680/geot.1999.49.3.387

Hird CC (1986) Stability charts for reinforced embankments on soft ground. Geotextiles and Geomembranes 4(2): 107-127. DOI: 10.1016/0266-1144(86)90019-1

Leshchinsky D, Reinschmidt AJ (1985) Stability of membrane reinforced slopes. Journal of Geotechnical Engineering, ASCE 111(11): 1285-1300. DOI: 10.1061/(ASCE)0733-9410(1985)111:11(1285)

Leshchinsky D, Boedeker RH (1989) Geosynthetic reinforced soil structures. Journal of Geotechnical Engineering, ASCE 115(10): 1459-1478. DOI: 10.1061/(ASCE)0733-9410(1989)115:10(1459)

Mandal JN, Labhane L (1992) A procedure for the design and analysis of geosynthetic reinforced soil slopes. Geotechnical and Geological Engineering 10(4): 291-319. DOI: 10.1007/BF00880706

Mandal JN, Joshi AA (1996) Design of geosynthetic reinforced embankments on soft soil. Geotextiles and Geomembranes 12:137-145. DOI:10.1016/0266-1144(95)00004-6

Mehdipour I, Ghazavi M, Moayed RZ (2013) Numerical study on stability analysis of geocell reinforced slopes by considering the bending effect. Geotextiles and Geomembranes 37: 23-34. DOI: 10.1016/j.geotexmem.2013.01.001

Mitchell JK, Christopher BR (1990) North American practice in reinforced soil systems. Design and performance of earth retaining structures, Special publication, ASCE 25:322-346.

Palmeira EM, Pereirab JHF, Silva AR L (1998) Back analyses of geosynthetic reinforced embankments on soft soils. Geotextiles and Geomembranes 16(5): 273-292. DOI: 10.1016/S0266-1144(98)00014-4

Sabhahit N, Basudhar PK, Madhav MR, Miura N (1994) Generalized stability analysis of reinforced embankments on soft clay. Geotextiles and Geomembranes 13(12): 765-780. DOI: 10.1016/0266-1144(94)00007-Z

Shahgholi M, Fakher A, Jones CJFP (2001) Horizontal slice method of analysis. Geotechnique 51(10): 881-885.

Tandjiria V, Low BK, Teh CI (2002) Effect of reinforcing force distribution on stability of embankments. Geotextiles and Geomembranes 20(6): 423-443. DOI: 10.1016/S0266-1144(02)00015-8

Wright SG, Duncan JM (1991) Limit equilibrium stability analyses for reinforced slopes. Transportation Research Record 1330, Transportation Research Board, Washington. D.C., USA. pp 40-46.

Zhang LY (2004) Development of software ZSLOPE for slope stability analysis. Chinese Journal of Rock Mechanics and Engineering 23(16): 2830-2835. (In Chinese)

Zhang LY (2005) Generalized limit equilibrium method for slope stability analysis. Chinese Journal of Rock Mechanics and Engineering 24(3): 496-501. (In Chinese)

Zhang LY, Zhang JM (2006a) Extended algorithm using Monte Carlo techniques for searching general critical slip surface in slope stability analysis. Chinese Journal of Geotechnical Engineering 28(7): 857-862. (In Chinese)

Zhang LY, Zhang JM (2006b) Modified Monte Carlo techniques by rotating slip segments for searching general critical slip surface (Ⅰ): Random angle of rotation. Rock and Soil Mechanics 27(11): 1902-1908. (In Chinese)

Zhang LY, Zhang JM (2006c) The extended Monte Carlo techniques by rotating slip segments for searching general critical slip surface (Ⅱ): Constant angle of rotation. Rock and Soil Mechanics 27(12):2197-2202. (In Chinese)

Zornberg JG, Sitar N, Mitchell JK (1998a) Performance of geosynthetic reinforced slopes at failure. Journal of Geotechnical and Geoenvironmental Engineering, ASCE 124(8): 670-683. DOI: 10.1061/(ASCE)1090-0241(1998)124:8(670)

Zornberg JG, Sitar N & Mitchell JK (1998b). Limit equilibrium as basis for design of geosynthetic reinforced slopes. Journal of Geotechnical and Geoenvironmental Engineering, ASCE 124(8): 684-698. DOI: 10.1061/(ASCE)1090-0241(1998)124:8(684)